

⁴E. L. Nagaev, *Fiz. Tverd. Tela* **4**, 2201 (1962) [*Soviet Phys. Solid State* **4**, 1611 (1963)].

⁵H. G. Reik, *Phys. Letters* **5**, 236 (1963); *Z. Physik* **203**, 346 (1967).

⁶H. G. Reik and D. Heese, *J. Phys. Chem. Solids* **28**, 581 (1967).

⁷M. I. Klinger, *Phys. Status Solidi* **11**, 499 (1965); **12**, 765 (1965); *Rept. Progr. Phys.* **31**, 225 (1968).

⁸P. Gosar and S. I. Choi, in *Excitons, Magnons and Phonons in Molecular Crystals*, edited by A. B. Zahlan (Cambridge U. P., Cambridge, England, 1968), p. 175.

⁹R. D. Puff and G. Whitfield, in *Polarons and Excitons*, edited by C. G. Kuper and G. D. Whitfield (Oliver and Boyd, Edinburgh, 1963), p. 171.

¹⁰R. Kubo, *J. Phys. Soc. Japan* **12**, 570 (1957).

PHYSICAL REVIEW B

VOLUME 3, NUMBER 6

15 MARCH 1971

Theory of the Effect of Finite Crystal Size on the Frequencies and Intensities of Impurity Absorption Lines in Semiconductors*

Bernard Bendow

University of California at San Diego, La Jolla, California 92037

(Received 9 November 1970)

It is demonstrated that when the dimensions of a semiconducting crystal are decreased to sizes of the order of the bulk impurity-electron Bohr radius a_0 , the impurity absorption edge abruptly shifts to higher energies, while the absorption intensity decreases abruptly (both within a few a_0). The larger the dielectric constant, the larger the dimensions at which the transitional behavior occurs. Various computed results are presented for an idealized model of a shallow impurity embedded at the center of various simple finite geometries.

INTRODUCTION

In semiconducting crystals, the impurity-electron¹ Bohr radius a_0 may exceed the interlattice spacing by as much as a few orders of magnitude,² depending on the values of the effective mass m^* and the dielectric constant ϵ ($a_0/a_H = \epsilon m_e/m^*$, where m_e is the electronic mass, and $a_H \sim 0.53 \text{ \AA}$, the free-hydrogen Bohr radius). So, although a thin semiconducting crystal may contain a large enough number of atomic layers to be described, at least approximately, in terms of bulk (infinite-crystal) properties, it may nevertheless be small enough to substantially alter the motion of impurity electrons. With recent progress in thin-film technology, and in view of the desirability of performing light-absorption experiments in such crystals,³ finite-size considerations should be of central importance in the interpretation of thin-film data, and, specifically, in deducing bulk properties from such data.

In the present paper we consider a very highly simplified model, where a single impurity is assumed fixed in the center of three specific geometries, illustrating cases where three, two, or one of the crystal dimensions are (is) finite, respectively: (a) sphere of radius R , (b) cylinder of radius R , and (c) thin film of half-width R . We employ an isotropic effective mass m^* and assume¹ a Coulomb interaction between electron and impurity. The purpose of the various simplifications is to allow the principal physical effects in such systems to emerge most clearly and directly, un-

hampered by unessential complications. The extension to generalizations such as nonisotropic mass, non-Coulomb interactions, or distributions of impurities should be evident from the development.

For purposes of definiteness let us from this point on speak in terms of a shallow acceptor¹ with binding energy $E_A = E_0$ in the bulk, bearing in mind that a parallel discussion follows as well for the donor case. Neglecting various broadening effects, impurity (assisted) absorption of light⁴ onsets when the photon energy ω satisfies $\omega = E_g - E_0$, where E_g is the energy gap. As $\omega \rightarrow E_g$ the absorption rate increases, undergoing a new onset (edge) at $\omega = E_g$ for unassisted absorption. As detailed in various places,⁵ this simplified picture can be directly generalized to include a series of impurity-electron states, as well as exciton effects. In our development we will not, for the most part, consider such effects: rather, we emphasize the impurity-electron ground state (gs) and its energy E relative to the gap E_g . For example, E_0 is the absolute value of E in the infinite crystal (binding energy or ionization energy). Note that in a finite crystal the term "binding energy" is misleading, as the gs energy E as defined here will now take on positive values; also, one does not have a continuum for energies above E_g as in the infinite crystal.

We are now in a position to point out two principle ways in which the impurity absorption is effected for $R \sim a_0$. First, the gs energy E is changed, so that the frequency at which absorp-

tion onsets changes. Second, the absorption rate per unit length, which is proportional to the square of the Fourier transform^{4,5} of the electron wave function evaluated at the photon wave vector \vec{k} , changes because the impurity-electron wave function changes. We assume that the band properties are not significantly changed⁶ when $R \sim a_0$. Considerations which arise when exciton effects are accounted for will be discussed later.

THEORY

We define $\vec{\rho} \equiv \vec{r}/a_0$, where \vec{r} is the electron-position vector measured from the impurity center. It is straightforward to show that the variational energy E/E_0 and variational ground state $\psi(\vec{\rho})$ are related as⁷

$$\frac{E}{E_0} = -\int_{\Omega} d\vec{\rho} \psi^*(\vec{\rho}) \left(\frac{\partial^2}{\partial \vec{\rho}^2} + \frac{2}{\rho} + V(\vec{\rho}) \right) \psi(\vec{\rho}) / \int_{\Omega} d\vec{\rho} \psi^*(\vec{\rho}) \psi(\vec{\rho}), \quad (1)$$

where Ω is the crystal volume and $V(\vec{\rho})$ is the total classical image potential energy^{6,8} of the electron-impurity system (in units of E_0), which includes interaction of the electron with both its own image and the impurity image, and the analogous quantities for the impurity. The various necessary image potentials follow directly from Maxwell's equations and the consequent boundary conditions.⁹ For the sphere one obtains directly

$$V_S(\vec{\rho}) = 2(\epsilon - 1) \sum_{l=1}^{\infty} \frac{(l+1)[(\epsilon+1)l+1]^{-1} \rho^{2l}}{\mathcal{R}^{2l+1}}, \quad (2)$$

where $\mathcal{R} \equiv R/a_0$. Similarly, we can express V for the thin film (leaving the result in integral form for compactness) as

$$V_F(\vec{\rho}) = 2\beta \int_0^{\infty} dk e^{-2k\mathcal{R}} (1 - \beta^2 e^{-2k\mathcal{R}})^{-1} \times \{ 2 [\cosh(2kz) + \beta e^{-2k\mathcal{R}}] + 2(1 + \beta e^{-2k\mathcal{R}}) \times [2 \cosh(2kz) J_0(ks) + 1] \}, \quad (3)$$

where, with the z axis perpendicular to the film,

$$z \equiv z/a_0, \quad s \equiv s/a_0, \quad (4)$$

$$s \equiv (x^2 + y^2)^{1/2}, \quad \beta \equiv (\epsilon - 1)/(\epsilon + 1),$$

and J is the Bessel function.

The net physical effect of the image potentials is repulsion of the electron from the crystal boundaries. We note that the kinetic energy is $\sim (\Delta x)^{-2}$ while the potential energy is $\sim (\Delta x)^{-1}$, where Δx is the effective electron range. This effect, coupled with the (positive) repulsive potential felt by the electron near the boundary, tends to increase E/E_0 , as will be reflected in the results which follow.

We introduce one further simplification, by assuming we may approximate the potential seen by the electron outside the crystal as being infinite. This assumption is employed and discussed by various other authors.^{5,8}

We employ the trial wave function, with variational parameters α_1 and α_2 ,

$$\psi^{\mathcal{R}}(\vec{\rho}, \alpha_1, \alpha_2) = \exp[-(\alpha_1 s^2 + \alpha_2 z^2)^{1/2}] \zeta^{\mathcal{R}}(\vec{\rho}), \quad (5)$$

where, denoting sphere by S , cylinder by C , and film by F ,

$$\zeta_S^{\mathcal{R}}(\vec{\rho}) = (1 - \rho/\mathcal{R}), \quad \zeta_C^{\mathcal{R}} = (1 - s/\mathcal{R}), \quad (6)$$

$$\zeta_F^{\mathcal{R}} = (1 - z/\mathcal{R}).$$

These wave functions correctly reduce to the infinite crystal form for $\rho \rightarrow \infty$, and obey the various necessary boundary conditions as well.

RESULTS

We first consider the dependence of E/E_0 on \mathcal{R} in the absence of an image potential ($V(\epsilon=1)$). In this case the sphere problem can be treated exactly by determining the zeros of solutions of the Laguerre equation¹⁰ for various values of \mathcal{R} . The cylinder and film, however, do not lend themselves to similar simplifications and must be treated variationally, as described above. The results of the computations are illustrated in Fig. 1(a); in all three geometries the transition from infinite to finite behavior occurs for $\mathcal{R} \sim 1-3$. The smaller the number of dimensions becoming finite, the smaller the value of \mathcal{R} at which the transition occurs, as would be anticipated from the kinetic-vs-potential energy discussion given previously.

Note that we limit our variational computations to values of E/E_0 less than zero; this is because the particular variational ψ chosen clearly becomes less and less accurate as $E/E_0 \rightarrow 0$. This may be seen from Fig. 1(b), where the spectrum of the sphere is labeled in terms of quantum numbers l , ν , where¹⁰

$$\psi \propto \rho^{\nu} e^{-\rho^2/\nu} L_{l\nu}, \quad (7)$$

where L is the solution of the Laguerre equation which corresponds to the Laguerre polynomials for ν integers. As ν increases from 2, our variational wave function ψ becomes a progressively worse trial wave function. In order to most properly continue the analysis to values of \mathcal{R} smaller than the transition value, ψ must be generalized; we do not do this here, but we bear in mind these limitations on the quantitative validity of the results when $E/E_0 \rightarrow 0$.

Figure 1(b) also illustrates the two lowest excited states for the spherical case for $\epsilon=1$, which correspond to the degenerate $2p$ and $2s$ states of

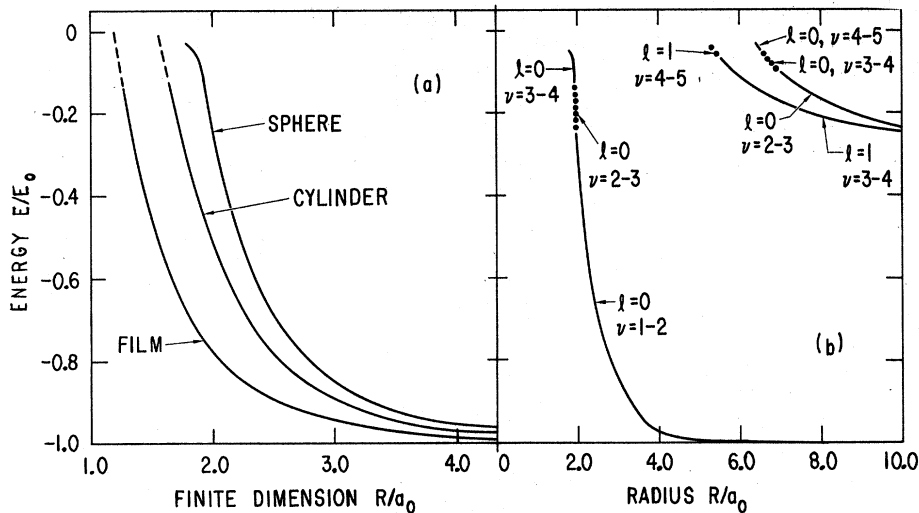


FIG. 1. (a) Energy E/E_0 vs the characteristic crystal dimension R/a_0 , for $\epsilon=1$, for three geometries detailed in the text. The sphere results are exact (nonvariational), the others variational. (b) Energy E/E_0 vs R/a_0 for a sphere with $\epsilon=1$, for the lowest three states. The states corresponding to various portions of the curves are indicated by quantum numbers l and ν arising in the Laguerre equation, as described in the text.

the infinite system. For these states which, however, have substantially lower absorption oscillator strengths ($\frac{1}{8}$ of the gs's in the infinite-crystal case) the effects of finite crystal size on E/E_0 occur already at substantially higher values of $R \sim 6-8$, although the decrease in $|E/E_0|$ with decreasing R proceeds much more slowly.

When the image potentials V of Eqs. (2) and (3) are now included in the computations, one obtains for E/E_0 vs R the results illustrated in Figs. 2(a) and 2(b), for the sphere and film, respectively. One notes the repulsive effect of the image potential; increasing ϵ (i. e., V) leads to an increase in E/E_0 . The variation of E/E_0 with ϵ is observed to be more pronounced for the film than the sphere. The dependence of E/E_0 on ϵ , for various values of R , is illustrated in Fig. 3 for the spherical case.

We now consider the effect of finite size on the absorption rate, which is proportional to $|\phi^{\alpha}(\vec{k})|^2$, where $\phi^{\alpha}(\vec{k})$ is the Fourier transform of $\psi^{\alpha}(\vec{r})$. For purposes of illustration, we consider $|\phi^{\alpha}(0)|^2$, an approximation to $|\phi^{\alpha}(\vec{k})|^2$ which is most appropriate near onset; and we define the ratio $F(R) \equiv |\phi^{\alpha}(0)|^2 / |\phi^{\infty}(0)|^2$ as a convenient means of comparing the finite- and infinite-crystal behavior.

By comparing the exact results for $\epsilon=1$ in the spherical case with variational ones, one can show that the two results for $F(R)$ are nearly equal for $R \gtrsim 2$. However, prudence prevents one from concluding that the use of the variational ψ 's are equally good in corresponding ranges of R for $\epsilon \neq 1$ and other geometries. Thus (excepting $\epsilon=1$ for the sphere) the variational portion of the results for F illustrated in Fig. 4 should be viewed only as qualitative indications of the actual behavior. In

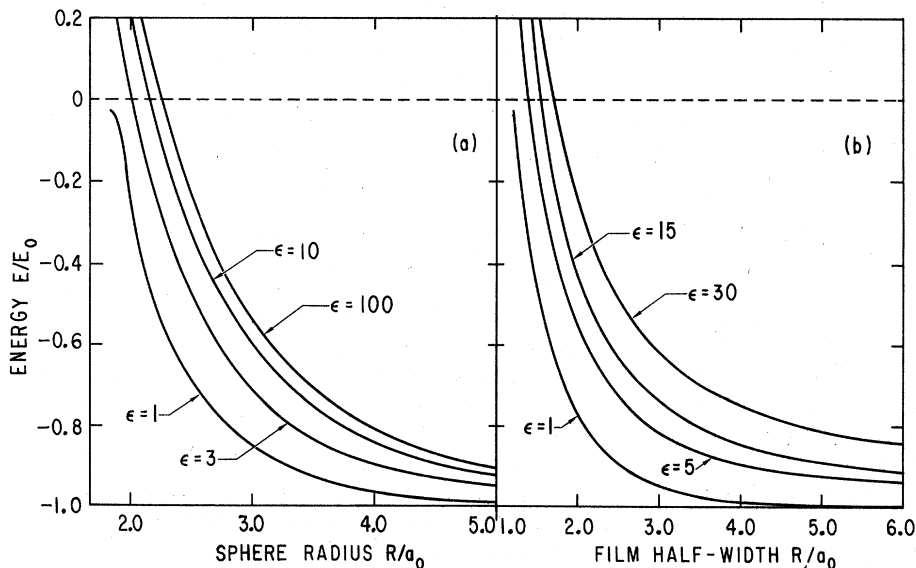


FIG. 2. (a) Energy E/E_0 vs radius R/a_0 for a sphere, for various values of the dielectric constant ϵ . Only $\epsilon=1$ results are exact (nonvariational). (b) E/E_0 vs half-width R/a_0 for film, for various values of ϵ .

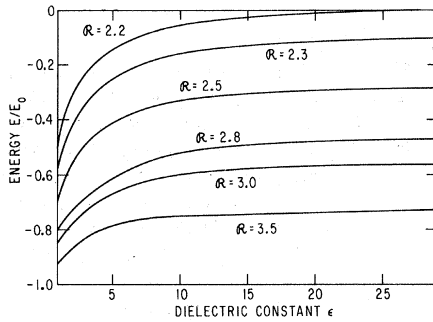


FIG. 3. Energy E/E_0 vs dielectric constant ϵ for various values of R ($\equiv R/a_0$), for sphere.

the present variational treatment, F turns out to be very weakly dependent on ϵ , so that the $\epsilon > 1$ results are nearly similar to those illustrated for $\epsilon = 1$. The present results are qualitatively similar to what one expects for free-exciton absorption,⁵ where $F \propto |\psi^{(0)}|^2$. In that case, higher E generally corresponds to states in which the electron spends less time near the origin (states with smaller oscillator strengths).¹¹ For example, for $l = 0$ in the bulk crystal, $|\phi(0)|^2 \propto n^{-3}$, where n is the principal quantum number. Here as well, for a given geometry and fixed value of ϵ , decreasing E and decreasing F go hand in hand, as a comparison of Figs. 2 and 4 indicates.

DISCUSSION

The results detailed above may be summarized briefly as follows:

Whenever the dimensions of a semiconducting crystal approach the bulk impurity-electron Bohr radius a_0 , the impurity absorption edge shifts toward higher energies, while the absorption rate decreases. The fewer dimensions becoming finite, and, for a given geometry, the smaller the dielectric constant ϵ , the smaller the value of the characteristic dimension(s) at which transitional behavior occurs. The transition region is fairly narrow, encompassing a few a_0 or less.

We now present a brief discussion of some related works. The theory of binding energies of shallow impurities on the plane surface of a semi-infinite semiconducting crystal has been given by various authors.⁸ The present procedures can be employed directly in conjunction with the latter work to extend the treatment to surface-state binding energies in crystals of finite size.

Studies of the energies of (unbound) excitons in thin films have been recently advanced.^{5,12} Shifts in the absorption lines with decreasing size have been observed¹² for excitons in MoS_2 . The film thickness was in a range where excited states, and not the gs, were the most substantially effected [cf.

Fig. 1(b)]. The theoretical treatment of Ref. 6 is appropriate to this higher range in R as well; good agreement is obtained there with the MoS_2 results. Variation in intensity with thickness was not discussed.

The present model is related qualitatively to the unbound exciton problem; the analogy may be shown to be best for the case where the hole mass greatly exceeds that of the electron. Formally, the present techniques are directly extendable to the exciton case when one includes the hole (impurity) kinetic energy and treats the full six-dimensional system dynamically; computationally, of course, the problem becomes significantly more involved. The qualitative similarity of the two problems, in any case, allows one to conclude that the experimental observations on unbound excitons imply the feasibility of observing identical effects in the impurity case. The exciton results indicate that for actual values of ϵ ($\neq 1$) the energy E does indeed take on positive values, so that our variational results for higher values of ϵ may in fact be acceptable for some range in $E > 0$.

We take note of various approximations and simplifications employed in the development. We have treated the impurity center statically because of its sizable mass. Also, we have considered only impurities in the center of various geometries, where the gs energy is minimal, thus determining the effective absorption edge when a nearly continuous distribution of impurities is present as well. That E is minimal for the impurity in the center may be understood in view of the heightened repulsion near surfaces in the present model. Even for $\epsilon = 1$ in a semi-infinite crystal, for example, the binding energy for a surface impurity is only 25% of the bulk value.

Other simplifications and possible generalizations are: (a) The theory is straightforwardly generalized to include n multiple levels with energies $E_g - E_n$ to which correspond sharp absorption edges

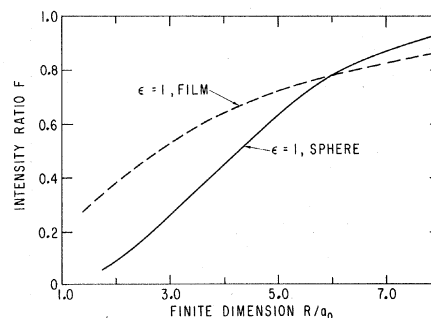


FIG. 4. Intensity ratio F vs R/a_0 for dielectric constant $\epsilon = 1$ for sphere (solid line) and for film (dotted line). Only sphere results are exact; film results are variational.

at these energies, in the absence of broadening. The edges and intensities vary for each level in a fashion similar to that emphasized here for the gs. (b) When (unbound) exciton effects are included, one has, superimposed on the broad-band impurity-assisted absorption, a set of discrete exciton lines¹¹ merging into a continuum at energy E_g , all corresponding to unassisted absorption. In the bulk, e.g., the ratio of acceptor-impurity to unbound-exciton energies is $(m_e^* + m_h^*)/m_h^*$, where m_e^* and m_h^* are the electron and hole effective masses. As the crystal dimensions are decreased, both sets of lines (or edges) shift simultaneously. Note, however, that the impurity mass greatly exceeds the hole mass of the exciton. Consequently, we expect (interactions aside) the uncertainty-principle energy of the order of \hbar^2/m^*R^2 which is associated with the exciton center-of-mass motion, to be much greater than its impurity-mass counterpart; but the larger the hole-to-electron mass ratio, and the larger is R , the less important is this particular distinction.

The shift in absorption edges with R provides a

possible experimental method of determining the average dimensions of microscopically powdered, fibrous, or layered materials. Conversely, a knowledge of the effects of finite size on the optical properties is requisite, should it be desired to employ powdered or similar forms of semiconducting materials in optical devices.

We conclude by suggesting that the substantial shifts in energy and decrease in intensities relative to the bulk values, which arise when crystal thickness is decreased to the order of the exciton Bohr radius, indicates that there may be points of diminishing returns in employing thinner and thinner crystals in optical-absorption experiments. Be that as it may, the theoretical considerations outlined here need to be incorporated whenever the experimenter desires to interpret his data in terms of bulk-crystal properties.

ACKNOWLEDGMENTS

The author thanks Walter Kohn, Erwin Mueller-Hartmann, and Herb Shore for useful discussions.

*Supported by the Office of Naval Research under Grant No. NONR-N00014-69-A-0200-6206, the Air Force Office of Scientific Research, Grant No. AFOSR 610-67, and the National Science Foundation, Grant No. GP-10943.

¹W. Kohn, *Solid State Phys.* **5**, 257 (1957).

²This may be seen employing the given expression for a_0/a_H , and noting that typical ranges are $\epsilon \sim 10-30$, $m^*/m_e \sim 0.01-1.0$, and lattice constants $a \sim 1-6 \text{ \AA}$. See, e.g., R. S. Knox, *Theory of Excitons* (Academic, New York, 1963); C. Kittel, *Introduction to Solid State Physics* (Wiley, New York, 1967), 3rd ed., and various references therein.

³Various well-known absorption experiments have proceeded at crystal thicknesses either of the order of, or approaching, sizes where the present effects occur. Some arbitrarily chosen earlier experiments are those discussed in *Semiconductors and Semimetals*, edited by R. K. Willardson and A. C. Beer (Academic, New York, 1967), Vol. 3, pp. 128, 136, and 221; lowest thicknesses were ~ 0.05 , 0.08 , and 4.4μ , respectively. A specific example of recently reported exciton data is: R. Z. Bach-

rach and F. C. Brown, *Phys. Rev. B* **1**, 818 (1970); lowest thicknesses were approximately a few hundred \AA .

⁴Various references are D. M. Eagles, *J. Phys. Chem. Solids* **16**, 76 (1960); H. J. Bowlden, *Phys. Rev.* **106**, 427 (1957); W. P. Dumke, *ibid.* **132**, 1998 (1963); and Ref. 1.

⁵See, e.g., Ref. 4, and the review article by E. J. Johnson in Ref. 3.

⁶G. Jones and J. L. Brebner, *Bull. Am. Phys. Soc.* **15**, 799 (1970); and private communication.

⁷See, e.g., A. Messiah, *Quantum Mechanics* (North-Holland, Amsterdam, 1962), Vol. II, Chap. XVIII.

⁸D. Schechter, *Phys. Rev. Letters* **19**, 692 (1967), and references therein.

⁹W. K. Panofsky and M. Phillips, *Classical Electricity and Magnetism* (Addison-Wesley, Reading, Mass., 1955), Chaps. 2 and 4.

¹⁰See, e.g., A. Messiah, in Ref. 7, Vol. I, Chap. XI.

¹¹R. J. Elliot, *Phys. Rev.* **108**, 1384 (1957).

¹²B. L. Evans and P. A. Young, *Proc. Roy. Soc. (London)* **298A**, 74 (1967).